

# An Error Model for Inter-Vehicle Communications in Highway Scenarios at 5.9GHz

Yunpeng Zang, Lothar Stibor  
Georgios Orfanos, Shumin Guo  
ComNets, RWTH-Aachen University

Kopernikusstr. 16  
52074 Aachen, Germany  
+49-(0)241-80-25829

{zyp|lsr|orf|gsm}@comnets.rwth-aachen.de

Hans-Juergen Reumerman  
Philips Research Laboratories Aachen

Weisshausstr. 2  
52066 Aachen, Germany  
+49-(0)241-6003-629

hans-j.reumerman@philips.com

## ABSTRACT

The design and evaluation of Inter-Vehicle Communication (IVC) protocols rely much on the accurate and efficient computational simulations. For simulations of Medium Access Control (MAC) and higher layers, the modeling work of underlying Physical layer (PHY) and wireless channel has impacts both on the computational efficiency of simulations and on the correctness of results. In this contribution, we discuss the modeling issues of the inter-vehicle wireless channel in highway scenarios and the packet error performance of Dedicated Short Range Communications (DSRC) PHY, which works at the newly allocated 5.9GHz Intelligent Transportation System (ITS) frequency band. A computationally efficient yet accurate enough error modeling approach used in our MAC layer simulator WARP2 is presented in this paper, together with simulation results. Both weaknesses and potential improvements of the proposed approach are discussed also in this work.

## Categories and Subject Descriptors

I.6.4 [Modeling Validation and Analysis]

## General Terms

Performance, Design

## Keywords

DSRC, IEEE 802.11p, ITS, Inter-Vehicle Communications, Wireless Channel model, Packet Error Ratio

## 1. INTRODUCTION

Inter-Vehicle Communications (IVC) and Vehicular Ad-hoc Networks (VANET) are becoming one of the most popular research topics in wireless communications, especially after the allocation of 75MHz spectrum at 5.9GHz in the U.S. for Intelligent Transportation Systems (ITS). Short range IVC technologies, like Dedicated Short Range Communications

(DSRC), are initially intended for the safety relevant applications such as local danger warning and vehicle collision avoidance. Due to the affluent spectrum resource, supports for non-safety relevant services, like inter-vehicle entertainments and on-road Internet access [1], are also under investigation for IVC.

The DSRC standard, which is being examined by the Institute of Electrical and Electronics Engineers (IEEE) 802.11p Task Group, is commonly accepted as one of the most potential technologies, which may dominate the future vehicular communication market. The DSRC specification uses a variation of the Orthogonal Frequency Division Multiplexing (OFDM) based IEEE 802.11a as the Physical layer (PHY), and a similar Medium Access Control (MAC) protocol to the IEEE 802.11 standard [2]. However, due to the fact that the inter-vehicle wireless channel is quite different from the one for indoor environments, which the original IEEE 802.11a PHY is designed for, the suitability and performance of DSRC/IEEE 802.11p PHY for the high mobility highway scenarios should be studied.

In this work we refer to the term *error model* as the packet error performance of the specific PHY in particular wireless environments. The error model is used for higher layer simulations as an abstraction of the underlying PHY and channel. Therefore the complexity and the accuracy of the error model will directly affect the simulation efficiency and correctness of the results.

Within the context of the WILLWARN (Wireless Local Danger Warning) application of the European Research project PREVENT [22], this paper is intended to present the computationally efficient error modeling approach used in our MAC layer simulator (WARP2) [3] for 5.9GHz IVC systems. The proposed error model is able to provide sufficient accuracy by taking account of the radio propagation characters and the PHY performance in real highway scenarios. Furthermore, the potential improvements and future work for the proposed approach are also discussed in the paper.

The paper is organized as follows: In Section 2 we survey the characters of inter-vehicle wireless channel in highway scenarios, based on which we review the DSRC/IEEE 802.11p PHY standard and analyze its suitability for the high mobility IVC in Section 3. The approach of the error model used in our WARP2 simulator is presented in Section 4. Section 5 gives simulation results achieved by using the presented error model. Limitation and further developments are discussed in Section 6 for the presented error model. Section 7 concludes the paper.

Permission to make digital or hard copies of all or part of this work for personal or classroom use is granted without fee provided that copies are not made or distributed for profit or commercial advantage and that copies bear this notice and the full citation on the first page. To copy otherwise, to republish, to post on servers or to redistribute to lists, requires prior specific permission and/or a fee.

PE-WASUN'05, October 10–13, 2005, Montreal, Quebec, Canada.

Copyright 2005 ACM 1-59593-182-1/05/0010...\$5.00.

## 2. INTER-VEHICLE RADIO CHANNEL IN A HIGHWAY ENVIRONMENT

As a basis of building the error model, the radio propagation characters of IVC are studied in this section.

The radio propagation characters are determined by many factors, such as operating frequency band, signal bandwidth, radio propagation environment, station mobility and antenna characters. For vehicular communications, the position of antennas, e.g., on the roof or at the front and rear bumpers of a car, has also impacts on the radio channel properties. In this work, we focus on the modeling of inter-vehicle wireless channel in a straight highway environment based the DSRC/IEEE 802.11p PHY, which has a signal bandwidth of 10MHz at 5.9GHz. Omni-directional antennas equipped on the top of vehicles are assumed in our work.

The effects introduced by the radio channel on the wireless signal can be interpreted as the combination of *large scale path loss* and *small-scale fading*. Large-scale path loss or path loss is used for predicting the mean signal strength for an arbitrary transmitter-receiver separation distance, while the small-scale fading characterizes the rapid fluctuations of the received signal strength over very short time duration, which are mainly the results from the signal's multi-path propagation and movement of the communicating vehicles. [5] Both path loss and small-scale fading have impact on the packet error performance of the target system. Studies in [6], [7], [8] and [9] have shown that both path loss and small-scale fading present different characters, depending on whether the direct Line Of Sight (LOS) path between the transmitter and receiver(s) exists or not. Thus, the channel should be modeled separately for the situations of LOS and Non-LOS (NLOS).

In a highway environment, the LOS path will exist if the communicating vehicles are right adjacent to each other or the traffic on the highway is sparse and no obstacle is present in between the transmitting and receiving antennas. In the LOS case the received signal can be interpreted as mainly composed of the directly received LOS path and a reflection off of the ground, which leads to the two-ray path loss model, as depicted in Figure 1. In [10], measurements were conducted for the inter-vehicle channel (without mobility) at 900MHz. The results imply the two-ray path loss model is more suitable for LOS cases. Studies in [11] and [12] also show that at 60GHz band the two-ray path loss model can give a quite precise prediction on the received mean power in the LOS case, when the vehicle are static or moving slowly. It has to be noticed that the measurements at 60GHz band are all carried out with the antennas located at the bumpers of vehicles. The Ricean distribution can be used for modeling the small-scale fading envelope of the received signal with the Ricean parameter K defining the ratio between the directly received power and the power of the reflected multipath rays.[5] The RMS delay spread values from 10ns to 40ns have been reported in [8] for the vehicle-to-vehicle communication with separation distances of 10 and 30 meters.

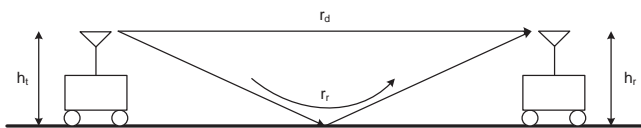


Figure 1. Two-ray path loss model

The NLOS case in a highway environment usually implies obstacles in between the transmitter and receiver(s), which happens most likely when the traffic load on a highway is heavy and the distance between the communicating vehicles is large. Authors in [13] reveal that the path loss model for IVC has dependence on the communication distance, instead of follows one model for all distance, especially in a crowded traffic scenario, e.g., in a traffic jam. Usually, the path loss in a NLOS can be modeled by the log-distance model with an exponent in range of 2.8 - 5.9 [6]. And the Rayleigh distribution can be used to model the small-scale fading [5].

In summary, the radio propagation characters in a highway environment are different for the LOS and the NLOS scenarios, which should be modeled separately. For the LOS case, the received power is dominated by the LOS path and the ground reflection path which can be modeled by the two-ray model. The RMS delay spread would be less than 50ns. This usually happens when the communicating vehicles are in adjacent to each other and the communication range is relative short, e.g., less than 35 meters [13]. For a longer communication range in a crowded traffic, it is more likely to have a NLOS scenario due to the block of LOS path by vehicles in between the transmitter and receivers. The RMS delay spread in NLOS scenario is much worse than in LOS scenario and can be up to 400ns.[14] The received signal can be modeled by the log-distance model for mean power and Rayleigh distribution for fading.

## 3. DSRC/802.11p PHY AND ITS SUITABILITY FOR HIGH-MOBILITY INTER-VEHICLE COMMUNICATIONS

In year 1999, the FCC of the US has allocated 75MHz bandwidth at 5.9GHz for the ITS applications. Seven 10MHz channels are planed in this band, as shown in Figure 2, consisting of one control channel and six service channels. DSRC has been adopted as the technique to offer ITS services on this frequency band. The DSRC/IEEE 802.11p PHY is a variation of the OFDM based IEEE 802.11a standard. The OFDM technique splits a high-rate data stream into a number of parallel lower rate streams and transmits them simultaneously over orthogonal frequency subcarriers.

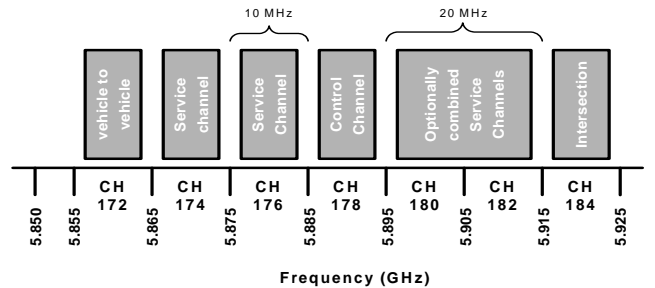
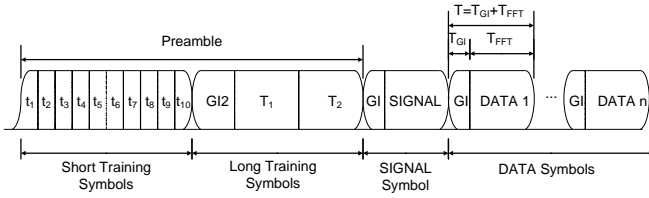


Figure 2. Frequency allocation of DSRC/IEEE 802.11p (The potentially combined 20MHz service channel (of two 10MHz channel) is also shown.)

The IEEE 802.11a PHY employs 64-subcarrier OFDM. 52 out of the 64 subcarriers are used for actual transmission consisting of 48 data subcarriers and 4 pilot subcarriers. The pilot signals are used for tracing the frequency offset and phase noise, and placed on subcarrier -21, -7, 7 and 21. The PHY data packet structure is depicted in Figure 3. The short training symbols, which are

located at the beginning of every PHY data packet (t1 through t10), are used for signal detection, coarse frequency offset estimation and time synchronization. The long training symbols (T1 and T2), which follow the short training symbols, are for the channel estimation and fine synchronization purposes. As shown in Figure 3, a guard time GI, i.e. cyclic prefix, is attached to each data OFDM symbol. The purpose of these cyclic prefixes is to eliminate the Inter Symbols Interference (ISI) caused by the multi-path propagation. But on the other hand, the cyclic prefixes bring down the system capacity and reduce the received effective Signal to Interference and Noise Ratio (SINR), since no useful information is carried by them. In order to combat the fading channel, information bits are coded and interleaved before they are modulated on subcarriers. Interleaving can spread the effect of the burst error over subcarriers in one OFDM symbol.



**Figure 3. IEEE 802.11a packet structure**

However, the IEEE 802.11a is designed for the high data rate multimedia communications in indoor environments with low user mobility. To make it work for high mobility vehicular communications, the DSRC/IEEE 802.11p PHY reduces the signal band from 20MHz to 10MHz. That means all parameter values are doubled in time domain comparing with the original IEEE 802.11a. Transmit power levels are adjusted in DSRC/IEEE 802.11p PHY to fit the requirements of outdoor vehicular communications. Except for these changes, the DSRC/IEEE 802.11p PHY and IEEE 802.11a are almost identical. Table 1 gives a brief comparison view on the DSRC/802.11p PHY and the original IEEE 802.11a.

**Table 1. Key Parameters of DSRC/IEEE 802.11p PHY and IEEE 802.11a PHY**

Parameters	DSRC/802.11p	802.11a
Information data rate Mb/s	3, 4.5, 6, 9, 12, 18, 24 and 27	6, 9, 12, 18, 24, 36, 48 and 54
Modulation	BPSK, QPSK, 16-QAM, 64-QAM	BPSK, QPSK, 16-QAM, 64-QAM
Coding rate	1/2, 1/3, 3/4	1/2, 1/3, 3/4
Number of subcarriers	52 (=48+4)	52 (=48+4)
OFDM symbol duration	8μs	4μs
Guard time	1.6μs	0.8μs
FFT period	6.4μs	3.2μs
Preamble duration	32μs	16μs
Subcarrier frequency spacing	0.15625MHz	0.3125MHz

Given the parameter values, we hereby analyze the suitability of DSRC/IEEE 802.11p PHY for high mobility vehicular communications.

As surveyed in Section 2, the worst RMS delay value can be  $\tau_{rms}=400ns$  in a NLOS case and the 50% coherence bandwidth will be approximately [5]  $B_c \approx 1/5\tau_{rms} = 500kHz$ , which is already on the order of subcarrier frequency. Although the prolonged guard time is sufficient to eliminate the ISI caused by the multi-path delay spread with a maximum value of  $1.6\mu s$ , the received signal may still suffer from the frequency selective fading. The reason is that the coherence bandwidth is smaller than the pilot spacing, which is around 2MHz (13 subcarrier spacings) in DSRC/IEEE 802.11p PHY, and the pilots are unable to accurately trace the frequency offset and phase noise. To solve this problem, a novel pseudo-pilot scheme is proposed in [15].

The impacts on the performance of PHY introduced by the high mobility can be investigated as the Doppler spread effect on the OFDM and the channel coherence time which limits the packet transmission length. For the worst case, e.g., two vehicles are moving with opposite directions, the maximum relative speed may be  $v=500km/h$ , which indicates a Doppler spread of:  $f_m=2.7kHz$ . On the one hand, the effect on OFDM caused by Doppler frequency spread can be ignored comparing with the clock drafting, which is around 118kHz assuming 20ppm oscillator accuracy and 5.9GHz carrier frequency. On the other hand, the channel coherence time will significantly affect the packet error performance, since packets are more vulnerable to the time-variant character of the channel in DSRC/IEEE 802.11p PHY. 2.7kHz Doppler spread indicates a channel coherence time of [5]  $T_c=0.423/f_m=157\mu s$ , which is the maximum packet length duration without being distorted during the transmission. This also indicates that the current training sequences, at the beginning of each packet, are not sufficient to estimate the channel correctly for a long packet.

To sum up, the DSRC/IEEE 802.11p PHY as a variation of 802.11a can efficiently mitigate the ISI introduced by multi-path delay spread. However, efforts are still needed to enhance the PHY against the frequency selective fading and the short channel coherence time in a high mobility environment.

#### 4. ERROR MODEL APPROACH FOR THE MAC LAYER SIMULATION

In this section we present the error modeling approach used in our MAC layer simulator Wireless Access Radio Protocol 2 (WARP2) [3] for the DSRC/IEEE 802.11p system.

Based on the calculation of SINR at each receiver, the arrived packets are determined to be successfully accepted or dropped. For a given SINR value, two error modeling approaches are most commonly used in network simulations [16]: the SINR threshold (SINRT) based method and Packet Error Ratio (PER) based method. With the SINRT based method, packet error is determined by directly comparing the received SINR with the SINRT. With PER based method, the packet error decision is made probabilistically based on the PER, which can be yielded from the theoretical calculation, link layer simulation or experimental measurement. Generally, it is considered that the PER based method is more realistic and more accurate than the SINR threshold method. However, with an enhanced channel

propagation model the SINR threshold method can also provide accurate modeling of the real PHY performance [17].

In WARP2 simulator we take the PER based solution, and the error modeling approach consists of following aspects:

- Modeling the radio propagation and determining the received signal power
- Calculating the effective SINR for each packet
- PER analysis or measurement for DSRC/IEEE 802.11p PHY

#### 4.1 Inter-vehicle channel model in WARP2 simulator

The received signal power is the basis of SINR calculation and determined by the transmission power and the radio propagation characters. In our approach, we care more about the received mean power, i.e. the effect of large scale fading, than small scale fading. This is because, on one hand, due to the use of channel coding and frequency interleaving, the bit error performance of an OFDM link in a frequency-selective channel depends more on the average received power than on the power of the weakest subcarrier [15], on the other hand, computational complexity dose not allow us to simulate the detailed small scale fading in a network simulation.

As studied in Section 2, the LOS and NLOS cases should be modeled separately due to the different radio propagation characters. For the LOS case we adopt the two-ray path loss model for determining the received signal power level [12]:

$$P_r = \frac{P_t G_t G_r}{L(r_d)} \left[ D_d \left( \frac{\lambda}{4\pi r_d} \right) + D_r \left( \frac{\lambda}{4\pi r_r} \right) \eta e^{-j\{k(r_d - r_r) + \phi\}} \right]^2 \quad (1)$$

where  $P_t$  is the transmit power,  $G_t$  and  $G_r$  are the gains of the transmitter and receiver antennas respectively,  $\lambda$  is the wavelength of the propagating signal,  $r_d$  and  $r_r$  are the optical path lengths of the direct and reflected waves, see Figure 1,  $\phi$  is the phase rotation during ground reflection,  $\eta$  is the reflection coefficient of the ground surface,  $D_d$  and  $D_r$  are the coefficients of antenna directivity,  $L(r_d)$  is the absorption factor, such as in atmosphere  $L(r_d) = (d/\lambda)^{\gamma-2}$ . With the assumptions of no antenna gain, same transmitter and receiver antenna heights and neglecting the antenna directivity and the distance between the traveling distances of the two propagation paths, equation (1) can be simplified to:

$$P_r = \frac{P_t}{(4\pi)^2 \left( \frac{d}{\lambda} \right)^\gamma} \left[ 1 + \eta^2 + 2\eta \cos \left( \frac{4\pi h^2}{d\lambda} \right) \right] \quad (2)$$

where  $\gamma$  is the path loss factor for LOS case.

For NLOS case, the log-distance path loss model [18] is employed:

$$P_r = \begin{cases} P_t G_t G_r \left( \frac{\lambda}{4\pi} \right)^2 & , d \leq 1m \\ P_t G_t G_r \left( \frac{\lambda}{4\pi} \right)^2 \cdot \frac{1}{d^\gamma} & , d > 1m \end{cases} \quad (3)$$

where  $d$  is the distance between the transmitter and the receiver, and  $\gamma$  takes value from 2.8 to 5.9.

In a highway scenario, the present of the LOS depends pretty much on the position of communicating vehicles and traffic situation around them. In order to simulate the real situation with a simplified complexity, we define two scenarios in the simulator, the crowded and the uncrowded scenarios. The uncrowded scenario implies a sparse traffic condition on the highway, vehicles can move with the relative high speed and the LOS path is less likely being blocked by intermediate vehicles. Therefore, the two-ray path loss model can be used for all communication ranges in this scenario. While in the crowded scenario, e.g. a traffic jam, the LOS path may exist only among the adjacent vehicles, and a longer communication range implies more vehicles in between the communicating pair and the LOS path being blocked with a higher probability. To further simplify the computational complexity, we define a threshold distance, which is used to separate the LOS and NLOS cases in the crowded scenario. The above discussed highway scenarios and corresponding channel models are listed in Table 2.

**Table 2. Channel models in a highway scenario**

Scenario	Path Loss Model	
Uncrowded	Two-ray model (LOS)	
Crowded	$d < \text{Threshold}$	Two-ray model (LOS)
	$d > \text{Threshold}$	Log-distance (NLOS)

$d$ : distance between the transmitter and the receiver.

#### 4.2 Calculation of the effective SINR for DSRC/IEEE 802.11p PHY

In this work, SINR is defined as

$$SINR = \frac{C}{\sum I + N} \quad (4)$$

where  $C$  is the signal level of the expected packet,  $\sum I$  denotes the sum of all interfering packet signal levels and  $N$  is the background noise.

Considering the fact that the arriving time of packets are totally asynchronous, especially when a contention based MAC protocol is used, we employ a simplified SINR calculation approach [18], as shown in Figure 4.

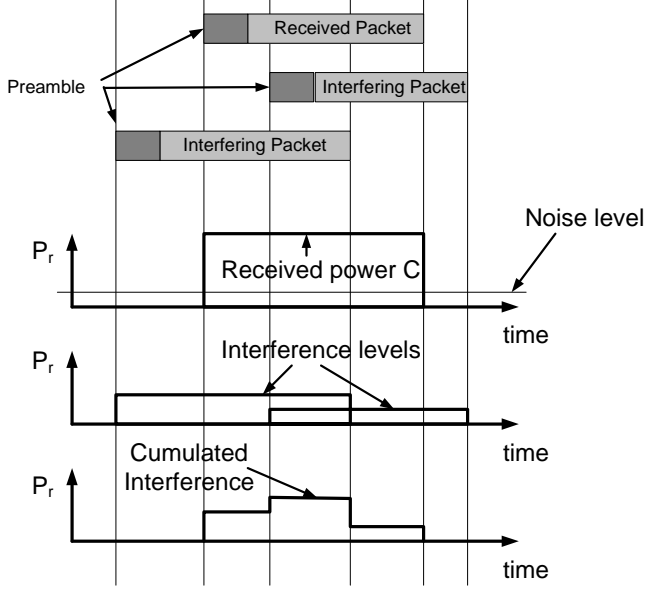


**Figure 4. Simplified SINR calculation**

SINR is calculated according to the length of the wanted packet. All interfering packet signals contribute to the interference part, but only for the overlapped duration, regardless earlier or later the interfering packets arrive than the wanted one. The cumulated effective interference energy is averaged over the wanted packet length before it is used for the SINR calculation. The received power is assumed to be constant through the whole length for every received packet. If there is another packet targeting at the receiver arrives during the reception of the wanted packet, the latter contributes only to the interference. Besides, if the cumulated interference level is too high, e.g., higher than the wanted signal level, the wanted packet will be dropped immediately.

Taking account of the effect introduced by the cyclical prefix attached to each OFDM symbol, the SINR should be reduced by a factor of  $\alpha$ , since no data information is carried by the cyclical prefix. [21] The value of  $\alpha$  is given by

$$\alpha = \frac{T_{IFFT}}{T_{IFFT} + T_g} \quad (5)$$

where  $T_{IFFT}$  is the Inverse Fast Fourier Transform (IFFT) period and  $T_g$  is the guard time, i.e. cyclic prefix length. In DSRC/IEEE 802.11p PHY,  $T_{IFFT}$  and  $T_g$  are  $6.4\mu s$  and  $1.6\mu s$ , respectively. Therefore, the  $\alpha$  value is 0.8, and the effective SINR, i.e.  $E_{av}/N_0$  used in next subsection, is calculated:

$$E_{av} / N_0 = \alpha \cdot \frac{C}{\sum I + N} \quad (6)$$

In summary, to apply this simplified SINR calculation we have made following assumptions:

- ISI has been eliminated by mean of attaching the cyclic prefix to each OFDM symbol.
- The correlation between the interference signals and wanted signal are neglected.

- The energy of an OFDM symbol is evenly distributed over all subcarriers, and due to the use of frequency interleaving all bits in a OFDM symbol suffer from the same  $E_{av}/N_0$ .
- Every packet has constant signal level over the whole packet duration, i.e., the Wide Sense Stationary (WSS) channel is assumed within the packet duration. This assumption also indicates that this SINR calculation method can not accurately simulate the big packet sizes in a high mobility scenario, where the channel coherence time may be smaller than the packet duration.

### 4.3 Error Probability Analysis of the DSRC/IEEE 802.11p PHY

In this subsection, we use the same approach as taken in [18] to calculate the upper boundary of the PER of DSRC/802.11p PHY based on the calculated SINR as described in Section 4.2.

According to the specification, the DSRC/802.11p PHY employs Binary Phase Shift Keying (BPSK), Quadrature Phase Shift Keying (QPSK), 16 Quadrature Amplitude Modulation (16QAM) and 64 QAM as the modulation schemes. Convolutional encoder with generator polynomials  $g_0=133_8$  and  $g_1=171_8$  is used for the generation of the basic rate of 1/2, from which other data rates are derive through puncturing.

#### 4.3.1 Bit Error Probability

The symbol error probability for an M-ary QAM can be calculated by [19]:

$$P_M = 1 - (1 - P_{\sqrt{M}})^2 \quad (7)$$

where

$$P_{\sqrt{M}} = 2 \cdot \left(1 - \frac{1}{\sqrt{M}}\right) \cdot Q\left(\sqrt{\frac{3}{M-1} \frac{E_{av}}{N_0}}\right) \quad (8)$$

and  $E_{av}/N_0$  is the average signal-to-noise ratio per symbol, which is obtained through the method described in Section 4.2, and the Q function can be found in [19]. For QPSK the symbol error probability is given by:

$$P_{QPSK} = 2Q\left(\sqrt{\frac{E_{av}}{N_0}}\right) \left[1 - \frac{1}{2}Q\left(\sqrt{\frac{2E_{av}}{N_0}}\right)\right] \quad (9)$$

In DSRC/802.11p PHY each OFDM data subcarrier carries one QAM symbol and the Gray coded constellation is proposed for modulation mapping. The bit error probability can be approximated by:

$$P_b \approx \frac{1}{\log_2 M} \cdot P_M \quad (10)$$

For BPSK modulation the bit error probability is the same as the symbol error probability, which is given by:

$$P_b^{(2)} = Q\left(\sqrt{2 \frac{E_{av}}{N_0}}\right) \quad (11)$$

### 4.3.2 Packet Error Probability

The evaluation of the packet error probability is complicated by the fact that the errors occur in burst, i.e. not independent, at the output of the Viterbi decoder, even if the errors in the decoder are independent [20]. Therefore, an upper bound for the packet error probability is given in [20]. For a packet of length of  $L$  bits which is transmitted with the PHY mode  $m$  the upper bound is:

$$P_e^m(L) \leq 1 - (1 - P_u^m)^{8L} \quad (12)$$

where  $P_u^m$  is union bound of the first event error probability given by:

$$P_u^m = \sum_{d=d_{free}}^{\infty} a_d \cdot P_d \quad (13)$$

$d_{free}$  in (13) is the minimal free distance of the convolutional code for the given code rate,  $a_d$  is the total number of errors with weight  $d$  and  $P_d$  is the probability of error in the pairwise comparison of two paths that differ in  $d$  bits. The values for  $a_d$  are obtained from the transfer function and represent the number of paths of distance  $d$  from the all-zero path.

When hard-decision decoding is applied,  $P_d$  is calculated by:

$$P_d = \begin{cases} \sum_{k=\frac{d+1}{2}}^d \binom{d}{k} p^k (1-p)^{d-k}, & d = \text{odd} \\ \sum_{k=\frac{d}{2}+1}^d \binom{d}{k} p^k (1-p)^{d-k} + \frac{1}{2} \binom{d}{d/2} p^{d/2} (1-p)^{d/2}, & d = \text{even} \end{cases} \quad (14)$$

where  $p$  is the bit error probability for the selected PHY mode  $m$ , and is given by (10) or (11).

Numerical calculations are carried out based on the analyses for the upper bound of bit error probability (Bit Error Rate BER) and packet error probability (Packet Error Rate PER) of DSRC/IEEE 802.11p PHY with different modulation and coding rates. In Figure 5, the packet error performance upper bounds of packet length 39, 375 and 2304 bytes are presented. The diagrams show that for each PHY model the PER is getting higher with the increasing packet length, and the PER dependency on packet length is in the range of 1.25dB between 39 and 2304 byte long packets.

However, for more accurate simulation results, the PER curves derived through specific link layer simulations [23] or field measurements should be used in stead of the analyzed upper bounds.

## 5. SIMULATION RESULTS

To illustrate the effects of the underlying error model upon the higher layer simulation results, in this section we present the results obtained through the WARP2 simulator based on the above mentioned modeling approach.

In the WARP2 simulator, the MAC and PHY protocols have been implemented according to DSRC/IEEE 802.11p specifications. The detailed MAC layer parameter values are listed in Table 3, while the PHY parameters can be found in Table 1.

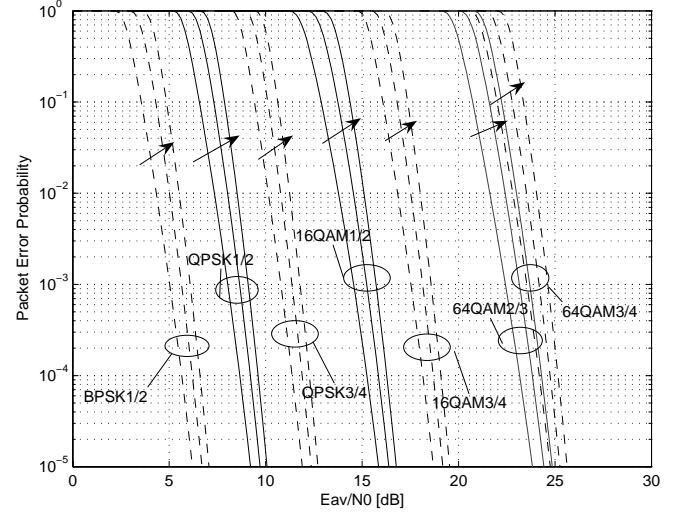


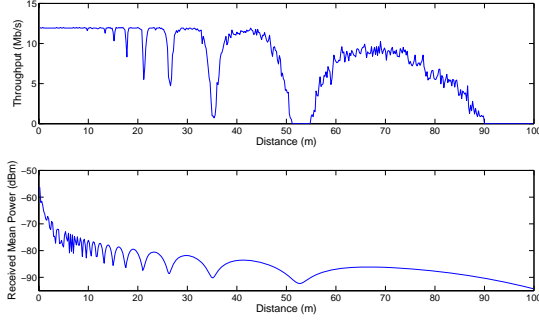
**Figure 5. Numerical results of PER with packet size 39, 275 and 2304. The arrow indicates the direction of packet size increasing.**

**Table 3. MAC parameters for the simulation**

Parameters	Values
CWMin	15
CWMax	1023
SlotTime	13μs
SIFSTime	32μs

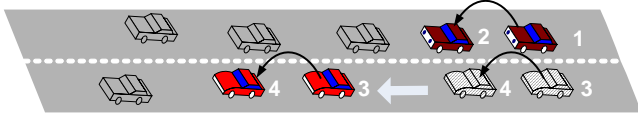
In the first simulation, a very simple scenario is set up to verify the impact of the channel model on the system throughput. In this scenario, two vehicles are moving on a highway and communicate with a simplex wireless link. The receiver is leaving the transmitter with a relative speed of 10m/s. The throughput values are evaluated with an interval of 0.2s corresponding to a moving distance of 2m.

Figure 6 shows the instant throughput result according to the distance between the transmitter and the receiver in an uncrowded scenario. In the simulation, no antenna gain is used, the gamma value takes 2.5 for the uncrowded scenario and the noise figure is  $-95\text{dBm}$ . The PHY mode 64QAM 3/4 is used with packet size of 200B, and immediate acknowledgement is employed in the MAC layer for the correct reception of packets. Transmission power is set to 20dBm. An overloaded Constant Bit Rate (CBR) traffic source is used at the transmitter in order to survey the maximum MAC layer throughput. It can be seen that the instant throughput changes according to the received mean power. However, due to the probabilistic decision at the receiver, the throughput value also fluctuates around the mean value. For 64QAM and 3/4 coding rate, the maximum MAC layer throughput can reach 12Mb/s, while the transmission range is limited within 100m.



**Figure 6.** Simulation results for 64QAM 3/4 with 0.1W transmit power in an uncrowded highway scenario. The upper is the instant throughput value, while the lower is the received mean power derived from the two-ray path-loss model.

The second scenario is intended to reveal another side of the effects introduced by the channel model. As shown in Figure 7, there are two communication pairs running on two adjacent lanes, vehicle 1 transmits to vehicle 2, and vehicle 3 transmits to vehicle 4.



**Figure 7.** In the second scenario, two communication pairs are leaving each other with a relative speed of 10m/s. Communication links are depicted by arrows.

The distances between each transmitter and receiver are fixed to 20m, while the second pair, i.e. vehicle 3 and 4, is moving apart from the first pair with a relative speed of 10m/s. The lane separation is 5m. Both communication links are using BPSK and 1/2 coding rate in the same channel with a packet size of 39B. The transmit power is set to 0.1W and no MAC layer acknowledgement is used for both links. Simulations with the same configuration were carried out for crowded and uncrowded scenarios, respectively. In the crowded scenario, the distance threshold for separating the LOS and NLOS cases is 35m, which indicates the signals will experience more serious attenuation and fading when the communication range is greater than 35m in a crowded scenario.

The throughput values of the two links in both crowded and uncrowded scenarios are shown in Figure 8. It can be seen that at beginning in both scenarios, each link can only get approximately half of the band width, while with the increasing distance between the two pairs each route can achieve higher throughput. This is mainly because the mutual interference between two communications links.

Comparing with the uncrowded scenario, the links in crowded scenario get to the maximum through earlier at 150m. This implies that on the one hand a higher attenuation can reduce the communication range, on the other hand, the system overall capacity can benefit from the spatial diversity induced by the attenuation.

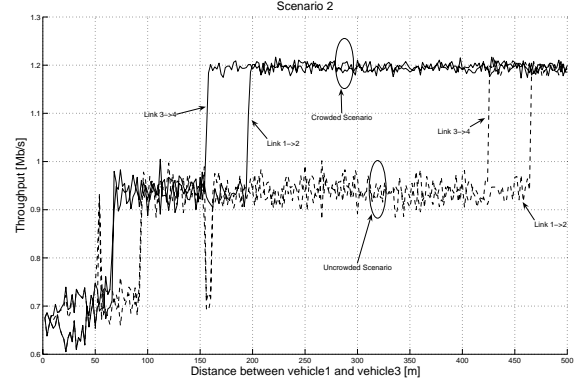


**Figure 8.** Link throughput in the crowded and uncrowded scenarios

## 6. DISCUSSION AND FURTHER WORK

The error model presented here takes into account the radio propagation properties in different traffic scenarios and the effects of packet length, modulation mode and coding rates. However, due to the simplification and assumptions made during the modeling process, there are several limitations on the proposed model:

- The effect of vehicle speed and impacts from the motion of surrounding objects are not addressed in this model.
- The differentiation of LOS and NLOS cases is highly abstracted in this model due to the complexity reason.
- More accurate simulation results need more precise packet error ratio values which can be gotten from the specific field experimental measurements.
- It remains to be investigated how to model the effects of frequency selective fading and channel coherence time in highway scenarios.

Therefore, further efforts towards a more accurate error model used for vehicular network simulations may concern:

- Intensive field measurements on the radio propagation characters and packet error performance specifically for the 5.9GHz DSRC based inter-vehicle communications in different scenarios.
- A more sophisticate mobility model that can provide more precise differentiation between the LOS and NLOS during the simulation.
- Enhancement to the DSRC/IEEE 802.11 PHY for improving its performance in high mobility highway environments.

## 7. CONCLUSION

In this paper, we surveyed the inter-vehicle wireless channel in highway scenarios and the suitability of DSRC/IEEE 802.11p PHY for such scenarios. A computational efficient error model used in our MAC layer simulator WARP2 is introduced for the study of DSRC/IEEE 802.11p based vehicular communications in highway scenarios. Both the numerical analyses for the packet error performance and the simulation results for DSRC system in



a highway environment are presented. The further development of the proposed error model is discussed as well.

## 8. ACKNOWLEDGEMENT

The authors would like to thank Dipl.-Ing. Guido Hiertz and Dr.-Ing. Juergen Maurer for their insightful advices and friendly support.

## 9. REFERENCES

- [1] Bhasker Reddy, J., Herremans, K., Van der Perre, L., Gyselinkx, B. and Engels, M. *Hybrid OFDM for future DSRC applications*. Vehicular Technology Conference, 2000. IEEE VTS-Fall VTC 2000. 52<sup>nd</sup>.
- [2] IEEE 802.11 WG, Part 11: Wireless LAN Medium Access Control (MAC) and Physical Layer (PHY) Specifications, IEEE, August 1999.
- [3] <http://www.comnets.rwth-aachen.de/~warp/>
- [4] Task3: Identify Intelligent Vehicle Safety Applications Enabled by DSRC-Interim Report, *Vehicle Safety Communications Consortium*, Jan. 2003.
- [5] T.S.Rappaport (Ed.), *Wireless Communications: Principle and Practice*, Upper Saddle River, NJ: Prentice-Hall, 1996.
- [6] Zhao, X., Kivinen, J., Vainikainen, P. and Skog, K. Propagation Characteristics for Wideband Outdoor Mobile Communications at 5.3 GHz. *IEEE Journal On Selected Areas In Communications*, Vol. 20, No. 3, April 2002.
- [7] Maurer, J., Fgen, T. and Wiesbeck, W. Narrow-band measurement and analysis of the inter-vehicle transmission channel at 5.2 GHz. *IEEE Vehicular Technology Conference*, 2002.
- [8] Batista da Silva, A. V. and Nakagawa, M. Radio wave propagation measurements in tunnel entrance environment for intelligent transportation systems applications. *2001 IEEE Intelligent Transportation Systems Conference Proceedings*, Oakland, CA, August 25-29, 2001.
- [9] Shimizu, H., Abo, M., Nagasawa, C. and Kobayashi T. Ray-Tracing Simulation of Path-Loss in Urban-Microcellular Environments under Road Traffic Conditions. *IEICE Trans. Commun.*, Vol. E87-B, No.1 Jan. 2004.
- [10] Davis, J. S. and Linnartz, Jean Paul M. G. Vehicle to Vehicle RF propagation Measurements. *1994 Conference Record of the Twenty-Eighth Asilomar Conference*, Volume: 1, Oct. 1994.
- [11] Mizutani, K. and Kohno, R. Analysis of multipath fading due to two-ray fading and vertical fluctuation of the vehicles in ITS inter-vehicle communications. *The IEEE 5th International Conference on Intelligent Transportation Systems*, 2002.
- [12] Kato, A., Sato, K. and Fujise, M. Technologies of Millimeter-Wave Inter-Vehicle Communications – Propagation Characters. *Journal of the Communications Research Laboratory*, 2001.
- [13] Takahashi, S., Kato, A., Sato, K. and Fujise, M. Distance Dependence of Path Loss for Millimeter Wave Inter-Vehicle Communications. In *Vehicular Technology Conference*, 2003. VTC 2003-Fall. 2003 IEEE 58<sup>th</sup>.
- [14] Yin, J., ElBatt, T., Habermas, S., Krishnan, H. and Talty, T. Performance Evaluation of Safety Applications over DSRC Vehicular Ad Hoc Networks. *Proceedings of the first ACM workshop on Vehicular ad hoc networks*, VANET, 2004.
- [15] Sibecas, S., Corral, C. A., Emami, S., Stratis. G. and Rasor, G. Pseudo-pilot OFDM scheme for 802.11a and R/A in DSRC applications. *Vehicular Technology Conference*, 2003. VTC 2003-Fall. 2003 IEEE 58<sup>th</sup>
- [16] Takai, M., Martin, J. and Bagrodia, R. Effects of Wireless Physical Layer Modeling in Mobile Ad Hoc Networks. *IEEE Journal On Selected Areas In Communications*, Vol. 21, No. 3, April, 2003.
- [17] Torrent-Moreno, M., Jiang, D. and Hartenstein, H. Broadcast reception rates and effects of priority access in 802.11-based vehicular ad-hoc networks. *Proceedings of the first ACM workshop on Vehicular ad hoc networks*, Oct. 2004.
- [18] Mangold, S. , Choi, S. and Esseling, N. An error model for radio transmissions of wireless LANs at 5GHz. *Proceeding Aachen Symposium 2001*, Aachen, Federal Republic of Germany, Sept. 2001
- [19] J. Proakis, *Digital Communications*. McGraw-Hill, Singapore, 4<sup>th</sup> Ed. 2001.
- [20] Pursley, M. B. and Taipale, D. J. Error probabilities for spread-spectrum packet radio with convolutional codes and Viterbi decoding. *IEEE Trans Communications*, vol. COM-35, no. 1, pp. 1-12, Jan 1987.
- [21] Tufvesson, F., Design on Wireless Communication Systems – Issues On Synchronization, Channel estimation and Multi-carrier Systems. Lund Sweden, KFS AB, 2000
- [22] PREVENT: Preventive and active safety; 6th Framework program integrated project <http://www.prevent-ip.org/>
- [23] Maurer, J., Fügen, T. and Wiesbeck, W. System Simulations Based on IEEE802.11a for Inter-Vehicle Communications Using a Realistic Channel Model. In *Proceeding of the 2nd International Workshop on Intelligent Transportation WIT2005*, Hamburg, Germany, Mar. 2005.